Lawrence Berkeley National Laboratory
Recent Work

Title
TOTAL ENERGY CALCULATIONS AND BONDING AT INTERFACES

Permalink
https://escholarship.org/uc/item/9v43c1ps

Author
Louie, S.G.

Publication Date
1984-08-01

eScholarship.org Powered by the California Digital Library
University of California

LBL-20792 c.2

Lawrence Berkeley Laboratory

UNIVERSITY OF CALIFORNIA

RECEIVED
LAWRENCE
BERKELEY LABORATORY
FEB 18 1986
LIBRARY AND
DOCUMENTS SECTION

Materials & Molecular Research Division

Presented at the International Conference on the Structure and Properties of Internal Interfaces, Irsee, West Germany, August 19-23, 1984; and to be published in Journal de Physique Coll. C4, 335 (1985)

TOTAL ENERGY CALCULATIONS AND BONDING AT INTERFACES

S.G. Louie

August 1984

TWO-WEEK LOAN COPY
This is a Library Circulating Copy which may be borrowed for two weeks.

LBL-20792 c.2

Prepared for the U.S. Department of Energy under Contract DE-AC03-76SF00098

DISCLAIMER

This document was prepared as an account of work sponsored by the United States Government. While this document is believed to contain correct information, neither the United States Government nor any agency thereof, nor the Regents of the University of California, nor any of their employees, makes any warranty, express or implied, or assumes any legal responsibility for the accuracy, completeness, or usefulness of any information, apparatus, product, or process disclosed, or represents that its use would not infringe privately owned rights. Reference herein to any specific commercial product, process, or service by its trade name, trademark, manufacturer, or otherwise, does not necessarily constitute or imply its endorsement, recommendation, or favoring by the United States Government or any agency thereof, or the Regents of the University of California. The views and opinions of authors expressed herein do not necessarily state or reflect those of the United States Government or any agency thereof or the Regents of the University of California.

TOTAL ENERGY CALCULATIONS AND BONDING AT INTERFACES

Steven G. Louie

Department of Physics, University of California,
and Lawrence Berkeley Laboratory, Berkeley, CA 94720

Abstract - Some of the concepts and theoretical techniques employed in recent *ab initio* studies of the electronic and structural properties of surfaces and interfaces are discussed. Results of total energy calculations for the 2x1 reconstructed diamond (111) surface and for stacking faults in Si are reviewed.

I - INTRODUCTION

A full understanding of a surface or interface requires knowledge of both its electronic and geometric structures. Hence, a great deal of effort has been devoted in the past decade in developing theoretical methods for calculating the properties and structure of interfaces from first principles. This paper describes some of the concepts and latest theoretical techniques used in addressing the interface problem. Several results obtained using the pseudopotential density functional method are presented to illustrate recent progress.

Much of the theoretical work in this area in the past has been focused on the electronic properties of the interfaces without consideration of their total energetics /1/. Thus, the geometric structures were necessary input to the calculations. The situation, however, is changing rapidly. In the last few years, it has become possible to calculate from first principles the detailed electronic and structural properties of materials and their surfaces. With basically the atomic number and atomic mass of the constituent atoms as input, many static and dynamical properties /2/ (e.g., cohesive energies, lattice constants, bulk moduli, phonon spectra, crystal structures, etc.) have been calculated to within a few percent of experiment. This development is made possible because of recent advances in the pseudopotential theory and total energy calculational techniques. It has opened up many exciting possibilities for the study of interfaces since there is little technical difference between a surface which is a vacuum-solid interface and a solid-solid interface. In this paper, we describe two recent applications of the theory as examples. One involves the prediction of the geometry of the diamond (111) surface /3/, and the other is a calculation of the properties of stacking faults in Si /4/.

The paper is organized in the following manner. In Sec. II, a short description of the theoretical methods is given. Section III presents a brief review of past self-consistent calculations in which only the electronic properties were considered. Results from two recent total energy calculations are presented in Sec. IV. The bonding properties and structure of the diamond (111) surface are discussed, and a minimum energy geometry for the 2x1 reconstructed surface is determined. Also presented is a study of the intrinsic and extrinsic stacking faults in Si. The stacking fault energies are obtained and found to be in good agreement with experimental values. The Hellmann-Feynman forces are calculated to study the forces on atoms near the faults. Localized defect (surface and fault) states are determined and their properties analyzed. Finally, Sec. V presents a summary.

II - THEORETICAL METHODS

The general approach involves reducing the many-body problem to that of a set of self-consistent field equations for the electrons. For ground-state properties, this is achieved, in principle, using the density functional formalism /5,6/. The eigenvalues of the resulting single-particle equations, the Kohn-Sham equations, are also often interpreted as excitation energies with reasonable results when analyzing the spectroscopic properties of material systems, although there is no formal justification for such association. The approach is *ab initio* in that the only input to the calculation is information about the constituent atoms and a set of possible structural topologies among which a minimal energy structure is derived.

The effective one-electron equations in this formalism are of the form (in atomic units):

$$\left\{-\frac{1}{2}\nabla^2 + V_{ext}(\vec{r}) + V_H(\vec{r}) + \mu_{xc}[n]\right\}\psi_i(\vec{r}) = \varepsilon_i\psi_i(\vec{r}) \tag{1}$$

where V_{ext} is the external potential seen by the electrons and V_H is the electrostatic or Hartree potential. μ_{xc} is the exchange-correlation part of the effective potential which is given by $\mu_{xc} = \delta E_{xc}/\delta n$ where E_{xc} is the exchange-correlation energy of the system. Finally, the density n is obtained from the one-particle wavefunctions

$$n(\vec{r}) = \sum_{i=1}^{N} |\psi_i(\vec{r})|^2 \tag{2}$$

where N is the number of electrons in the system. What remains is the specification of E_{xc}. Since the exact functional is not known, the most widely used scheme is the local density approximation (LDA)/6/:

$$E_{xc}^{LDA} = \int d\vec{r}\; n(\vec{r})\; \varepsilon_{xc}^{hom}(n(\vec{r})) \tag{3}$$

where $\varepsilon_{xc}^{hom}(n)$ is the exchange-correlation energy density of the homogeneous electron gas of density n. Several parameterizations of electron gas data are in common use.

In the pseudopotential approach, the solid is considered to be composed of rigid ion cores and the valence electrons which are itinerant. The self-consistent field equations are carried out only for the valence electrons. The external potential V_{ext} due to the cores are modeled by superposition of ionic pseudopotentials which are constructed from a knowledge of only the atomic numbers. The electron wavefunctions are obtained by solving the Kohn-Sham equations using a basis set expansion in either plane waves or localized orbitals.

Once the one-electron wave equation has been solved, the total energy of the system may be evaluated by adding the core-core and electron-electron interaction energies to the core-electron interaction energy /7/. The total energy is usually cast in the form

$$E_{total} = \sum_{i=1}^{N} \varepsilon_i - \frac{1}{2}\int V_H(\vec{r})n(\vec{r})d\vec{r} - \int \mu_{xc}[n]n(\vec{r})d\vec{r} + \int \varepsilon_{xc}[n]n(\vec{r})d\vec{r} + E_{ion-ion} \tag{4}$$

where the sum is over all occupied states and $E_{ion-ion}$ is the electrostatic interaction energy among the bare ions. Once the lowest energy structure is found, the other solid state properties can be computed.

An interface being a defect to an otherwise perfect crystal poses additional constraints to the calculations. One is the lack of translational symmetry because of the interface. This can be overcome in two ways. One approach is to match wavefunctions across the interface allowing both extended and decaying states.

Another is to use the so-called supercell method in which the interface is repeated indefinitively with certain separation to prevent interaction between interfaces. This method allows the use of standard band structure techniques since periodicity is mathematically restored. It is the most common and is the method employed for the studies discussed here. Another constraint in interface studies is the requirement of detailed self-consistency in the calculations because of the possibly important charge rearrangement near the interface. Quantities such as atomic rearrangements and interfacial formation energies are sensitive to such charge rearrangements.

III - SELF-CONSISTENT CALCULATIONS

In the 1970's, many surfaces and interfaces were studied using the self-consistent pseudopotential method /1,8/. In these studies, the electronic structure was calculated self-consistently for an assumed structure. However, no attempt was made to compute the lowest total energy structure because of theoretical and computational difficulties. Thus, in the scheme described in Sec. II, the steps for total energy evaluation were not carried out. The atomic positions were either inferred indirectly from experiments or taken to be those of idealized models. Nevertheless, from these electronic structure calculations, a great deal has been learned about surfaces and interfaces, and the results often provided the needed interpretations and explanations of experimental observations.

These self-consistent pseudopotential studies included metal and semiconductor surfaces, metal-semiconductor interfaces (Schottky barriers), semiconductor-semiconductor interfaces (heterojunctions), and stacking faults. In this section, we briefly describe one application to illustrate some of the theoretical concepts and techniques used in studying interfacial systems and also the limitations of the approach without total energy and force information.

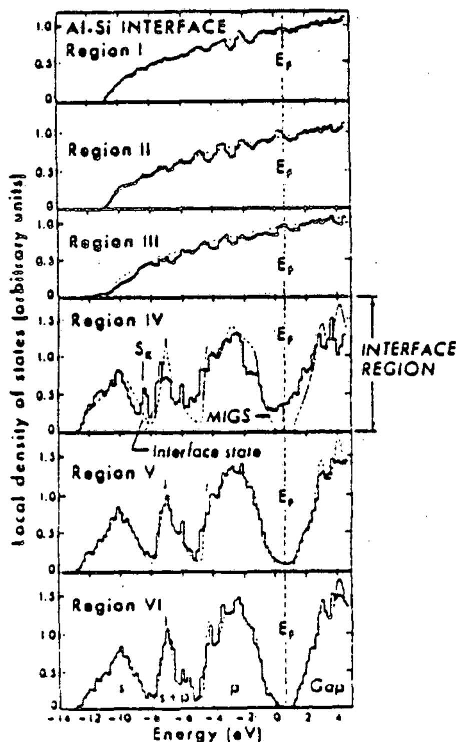

Fig. 1 - Local density of states near an Al/Si(111) interface. (arbitrary units)

For a given structure, the calculations yield a host of information on the electronic properties including the interface energy bands, charge densities, local densities of states, and so forth. The calculated local density of states (LDOS) which describes the electron energy spectrum as function of position in real space for an Al/Si(111) interface /9/ is presented in Fig. 1. In this work, the supercell consisted of 12 layers of the silicon crystal along the (111) direction and an equivalent thickness of Al which was approximated by the jellium model since the exact geometry at the interface is not known. The edge of the jellium is taken to be at a distance of one-half the Si-Si bond length. The unit cell, thus, is composed of an Al half and a Si half, and each is divided into three regions for the purpose of analyzing the LDOS. As shown in Fig. 1, the LDOS changes from that of a free-electron model of a metal with a square root dependence on energy in region I, which is deep in the Al side, to that of bulk Si in region VI which is the Si region farthest from the interface.

Region IV is the transition region on the Si side and is the most interesting region.

Unlike the bulk LDOS, new metal-induced gap states (MIGS) appear in the Si band gap in this region. These states are bulk-like in the metal, have large amplitude in the dangling bond sites of the Si surface, and decay rapidly into the semiconductor /9/. It is these states which determine the Schottky barrier properties. Localized interface states which decay in both directions away from the interface also exist for this system. The peak in the valence band (labeled S_k) at -8.5 eV arises from such localized states. Because these states are deep in the valence band, they do not contribute to the transport properties of the Schottky barriers. From the Fermi level and the position of the conduction band minimum, the barrier height can be evaluated as seen in Fig. 1. The calculated value is 0.6 ± 0.1 eV which is in very good agreement with the measured value of 0.6 eV /10/.

The MIGS in the band gap are Si dangling bond surface states hybridized with the continuum states of the metals. They are, therefore, hybrid states which are intermediate between the Bardeen (surface state) and the Heine (metallic tail state) pictures /11/. At the interface, the formation of the MIGS and the subsequent dipole potential created due to the occupation of them equalize the Fermi levels of the two materials and determine the Schottky barrier height. Similar calculations were done for the III-V and II-VI compound semiconductor-metal interfaces /12/. The same qualitative picture emerged with the trend that both the density of MIGS and the penetration of the MIGS into the semiconductor decrease as the ionicity or the band gap of the semiconductor increases. This is intuitive since a bigger band gap implies a larger effective barrier for these states to penetrate into the semiconductor. With the MIGS as a conceptual basis, a microscopic theory for the behavior of the Schottky barrier has been constructed which, for example, explains the change in barrier height with metal electronegativity /12/.

The above example serves to illustrate both the power and limitation of the self-consistent pseudopotential method. Although we have learned much about the general electronic nature of metal-semiconductor interfaces, we have not gained information on the detail geometric structure or chemical bonding at the interface. Since experiments still cannot reliably yield interfacial structures, this is a major deficiency for methods which must rely on experimentally determined geometries or idealized models.

IV - TOTAL ENERGY CALCULATIONS

In the *ab initio* total energy calculations, the exact geometry is no longer a required input. The structure is determined by minimizing the total energy with respect to the atomic coordinates near the interface for a given topology. Alternatively, the Hellmann-Feynman forces on each atom are calculated, and the atoms are moved until all forces are zero. In either approach, the calculation must be done iteratively since new forces develop on their neighbors when atoms are moved. Several cycles are usually needed to achieve a minimum energy, zero force structure. In this approach, both electronic and structural properties are obtained.

Several important factors contributed to the development and use of *ab initio* total energy calculations in the 1980's /2/. Among these are the refinements in band structure calculational techniques, development of approximations to the density functional formalism, invention of the *ab initio* pseudopotentials, and development of techniques for calculating total energies and forces. In this section, we review two calculations using this approach--the diamond (111) surface as a prototype vacuum-solid interface for tetrahedral covalent materials and the intrinsic and extrinsic stacking faults along the [111] direction in Si as examples of internal interfaces.

A. Diamond (111) Surface

The determination of surface structure is a major unsolved problem in surface science. No definitive experimental probe has been developed yet for giving detailed surface geometry. There are many models proposed to explain the experimental data for the diamond (111) surface as well as for many other surfaces. *Ab initio* total

Table I. Ground-state properties of diamond and Si.

	Lattice Constant (Å)	Cohesive Energy (eV/atom)	Bulk Modulus (Mbar)
Diamond			
Theory	3.56	7.84	4.37
Experiment	3.57	7.37	4.42
Silicon			
Theory	5.41	4.76	0.93
Experiment	5.43	4.63	0.99

energy calculations should be able to distinguish among these models and suggest a possible low energy structure.

Table I summarizes some of the structural properties of bulk diamond calculated using a liner combination of atomic-like (Gaussian) orbitals basis set /13/. This basis set is employed because of the localized nature of the carbon electron wavefunctions. Three Gaussian exponents for each of the s, p_x, p_y, and p_z orbitals totaling 12 basis functions per carbon atom were used. The results illustrate the accuracy of the method and serve as calibrations for the surface study. The computed lattice constant, cohesive energies, and bulk modulus are all in excellent agreement with experimental values.

The diamond (111) surface is of interest as the insulating limit for the group IV (111) surfaces which show a remarkable variety of surface reconstructions, that is, atomic rearrangements which result in a change in the ideal surface symmetry. Recent experiments indicate a hydrogen-terminated 1x1 surface at room temperature, but the 2x1/2x2 surface seen by Low Energy Electron Diffraction (LEED) for surfaces cleaned by annealing to above 1000 C is apparently H-free /14-17/. (LEED cannot distinguish between a true 2x2 or disordered domains of 2x1 for this surface; the similarity of the angle-resolved photoemission to that of the 2x1 Si(111) and Ge(111) surfaces suggests the latter.) Although there are many models proposed for this surface, the correct structure remains undetermined. In the study /3/, energy minimization is carried out for all the topologically distinct 2x1 models in the literature. These models are all motivated by experimental data such as those from LEED or angle-resolved photoemission experiments. The structures considered include the ideal relaxed model, the Haneman buckling model /18/, the Pandey π-bonded chain model /19/, the Chadi molecule model /20/, and the Seiwatz single chain model /21/. (See Fig. 2.)

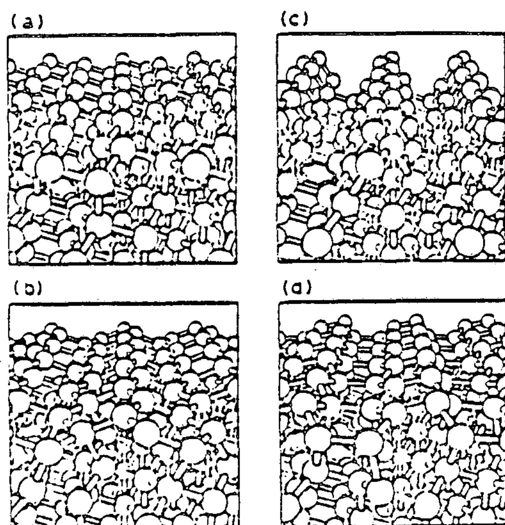

Fig. 2 - Geometries of 1x1 and 2x1 diamond (111) surfaces: (a) ideal structure, (b) Pandey chain model, (c) Seiwatz single chain model, and (d) Chadi molecule model.

The calculated total energies for these models are summarized in Table II. The energy per surface atom for the ideal 1x1 model is used as zero of energy. Relaxing the first two surface bonds (Fig. 3(a)) lowers the energy by 0.37 eV. Buckling of the 1x1 surface by raising and lowering alternate rows of surface atoms, on the other hand, is found to raise the energy. Of the other three 2x1 models, the ideal Pandey chain model /22/ has the lowest energy. The Seiwatz single chain model is clearly unfavorable, and the Chadi molecule model, which has the second lowest energy, has not been relaxed further because the calculated surface state dispersion is inconsistent with angle-resolved photoemission data /14/.

The energy of the Pandey model is further minimized by adjusting the four surface-most bond lengths to give the

Table II. Calculated total energies of C(111) 1x1 and 2x1 surface reconstruction models.

Surface model	Energy eV/(surface atom)
Ideal 1x1	0.00
Relaxed 1x1	-0.37
Buckled ($\Delta z = \pm 0.26$ A)	0.35
Chadi π-bonded molecule	0.28
Seiwatz single chain	1.30
Ideal Pandey π-bonded chain	-0.05
Relaxed Pandey π-bonded chain	-0.47
Same with ±2% dimerization	-0.46
Same with ±4% dimerization	-0.43
Same with ±6% dimerization	-0.38
Fully relaxed Pandey chain	-0.68

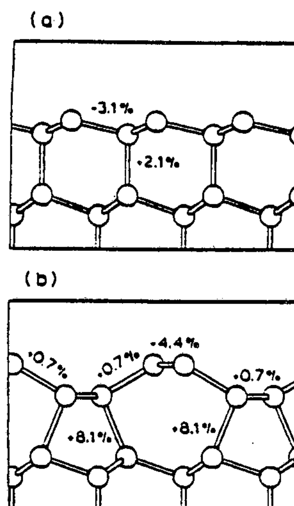

Fig. 3 - Bond length changes (with respect to bulk) of (a) relaxed 1x1 and (b) relaxed 2x1 Pandey chain models for the diamond (111) surface.

"relaxed" structure of Fig. 3(b) lowering the energy to -0.47 eV. A rather unexpected feature of the resulting geometry is the 8% lengthening of the subsurface interlayer bond. In contrast, the surface chain bond was only shortened by 4% to a length which is approximately midway between that of graphite and diamond. Another important result is that, contrary to some speculations, dimerization of the chain is found to raise the surface energy. The structure can be further relaxed by allowing the atoms below the first two layers to move. This movement relieves some of the bond angle strains on the third layer atoms. The final fully relaxed structure has an energy lowered by an additional 0.21 eV per surface atom.

Once a minimum energy structure is determined, the calculated surface state dispersion can be used to compare with experimental results for confirmation. Figure 4 shows the calculated surface band structure for the fully relaxed Pandey chain model with the Fermi level at near 2 eV. Experimental angle-resolved photoemission data /14/ for the occupied surface states are shown for comparison. There is good agreement between theory and experiment for the band dispersion. However, the calculated band is too high by a rigid shift of ~1 eV. This kind of discrepancy is most likely caused by using the local density approximation which is well-known to give excellent structural (ground-state) properties but too small excitation energies Similar calculations /23/ have been carried out for the 2x1 phases of the (111) surfaces of Si and Ge. The results obtained are qualitatively the same. Namely, the relaxed π-bonded chain geometry yields the lowest total energy among the structures tested, and the surface band dispersions are in good agreement with experiment but not the band positions.

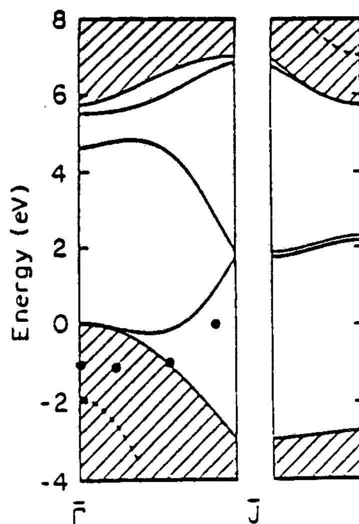

Fig. 4 - Calculated surface bands (solid lines) and resonances (dashed lines) for the 2x1 diamond (111) surface for fully relaxed Pandey chain model. Black dots are experimental data of Ref. 14.

From these results, the structure and bonding at this surface can be described in

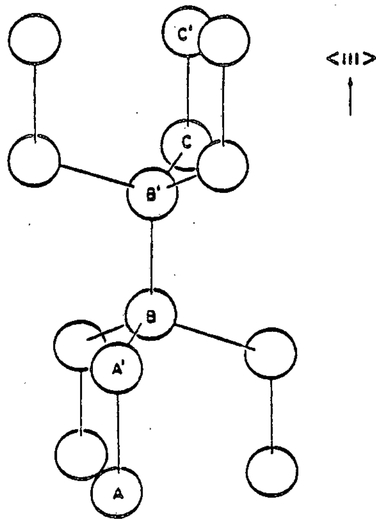

Fig. 5 - Geometry of the diamond structure.

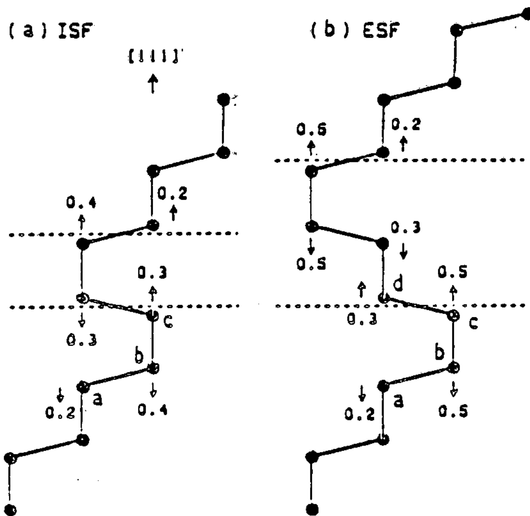

Fig. 6 - Atomic positions in the (110) plane of Si for (a) ISF and (b) ESF. The dashed line indicates a stacking fault plane. The net force on each atom in this ideal geometry is marked in units of 10^{-2} Ry/a.u.

the following terms. The driving mechanism for the reconstruction is the existence of half-occupied dangling bonds of the ideal (111) surface which are highly unfavorable energetically. In the π-bonded chain geometry, the surface is stabilized by allowing the dangling bonds to move into near-neighbor positions where they can participate in π bonding. However, this geometry results in large bond angle distortions which give rise to a strain energy. The second and third layer atoms are, thus, forced to move to relieve the strains resulting in a final relaxed geometry. The same general mechanism appears to be operative for the (111) surfaces of all three of the group IV elements.

B. Stacking Faults in Si

Stacking faults are probably the simplest of the planar defects or internal interfaces. For diamond structure semiconductors, stacking faults along the [111] direction correspond to a misplacement of the third nearest-neighbor arrangement, and the systems are only slightly disturbed compared to those due to other bond-breaking defects. There are, however, rather few theoretical investigations of the stacking faults in semiconductors. In particular, there has not been a complete study for the total energy or the structure of Si stacking faults in the literature.

Experimentally, the inferred stacking fault energies for Si are very small (about 50-60 erg/cm^2) /24,25/. A recent charge collection scanning electron microscopy experiment on an extrinsic stacking fault in n-type silicon suggested the existence of stacking fault states with energies at about 0.1 eV below the conduction band minimum /26/. Photoluminescence spectra of plastically deformed samples showed a defect state near 0.15 eV above the valence band maximum /27/.

The stacking sequence along the [111] direction in the diamond structure is AA'BB'CC. (See Fig. 5.) An intrinsic stacking fault (ISF) is a planar defect corresponding to a pair of atomic planes missing from the ideal stacking sequence, and an extrinsic stacking fault is a defect resulting from adding a pair of atomic planes (e.g., AA' inserted between BB' and CC'). The atomic positions near the faults in the (110) plane are shown in Fig. 6. For both types of faults, the orientation of the Si-Si bond is rotated 120° from its normal direction when passing through a fault plane (dashed line in Fig. 6). As a consequence, for the atoms near a fault (e.g., atom a in Fig. 6(a) and atoms a and d in Fig. 6(b)), the numbers of first and second nearest neighbors are not changed, but the number of third nearest neighbors is reduced from 12 to 9 with one additional neighboring atom at a distance slightly larger than the second nearest-neighbor distance.

In the calculation /4/, the geometries shown in Fig. 6 are used to calculate the total energies of the ISF and the ESF. Supercells of 10 (14) atoms are constructed for the ISF (ESF). The total energies of the perfect crystal and that of the crystal with stacking faults are compared to obtain the stacking fault energies. Since we are calculating extremely small energy differences, great care is needed in treating the perfect crystal and the supercells with the faults in equal footing numerically so that the required precision is obtained. The calculations are carried out using a plane wave basis with $(\vec{k}+\vec{G})^2$ up to 10 Ry which corresponds to about 70 plane waves per atom.

Table I displays some of the calculated static structural properties of the Si perfect crystal using a six-atom supercell of the same symmetry as the supercells containing the stacking faults. The calculated lattice constant is 5.41 A, which is in excellent agreement with the experimental value of 5.43 A. All subsequent results are obtained at this calculated equilibrium lattice constant. The calculated stacking fault energy is 40 erg/cm^2 and 26 erg/cm^2 for the ISF and ESF respectively. The uncertainty in the theoretical values resulting from the finite number of planes waves and $\vec{k}$ points is estimated to be 20%. The experimental values /24,25/ which are extracted using elasticity models vary from 50 to 70 erg/cm^2 for the ISF and from 50 to 60 erg/cm^2 for the ESF. Thus, the theory is in reasonable agreement with experiment. Although there has been previous theoretical work /28-30/, this is the first time that stacking fault energies are obtained from an ab initio self-consistent calculation.

In addition to the fault energies, forces are calculated using the Hellmann-Feynman theorem. This provides information on the tendency of the atoms to relax near the fault. The force on each atom near the faults in the ideal geometry are shown in Fig. 6. The three-fold rotational symmetry around the [111] axis dictates that the only forces existing are along the [111] direction. As seen from the figure, atoms belonging to the same double layer immediately next to a fault plane (e.g., atoms b and c) tend to lengthen the covalent bond between them. Also, the atoms belonging to different double layers (e.g., atoms a and d in Fig. 6(b)) also tend to repel each other. The net effect is that the mis-oriented bonds along the chain want to move away from the bond directly below or above it. Thus, these results predict that the fully relaxed structure for both ISF and ESF would be slightly dilated along the [111] direction.

The calculated energy bands in the two-dimensional Brillouin zone are presented in Fig. 7 for the ISF. The allowed bulk states (the projected band structure) are given by the shaded regions. Stacking fault states (dashed lines) are found in the gap region near $\bar{\Gamma}$ and $\bar{K}$. There are two fault states at $\bar{\Gamma}$ for the ISF. One is a two-fold degenerate state at about 0.1 eV above the valence band maximum; the other is singly degenerate at about 0.3 eV below the conduction band minimum. The charge density of these states is plotted in Fig. 8. The state near the valence band maximum is a bonding state with charge density mainly concentrated between fault atoms (Fig. 8(a)). The level position of this state is consistent with the photoluminescence spectrum finding /27/. The state below the conduction band minimum at $\bar{\Gamma}$ is, on the other hand, an anti-bonding state

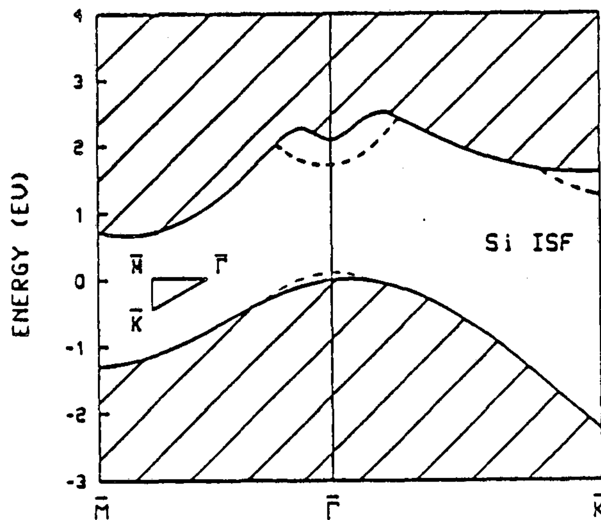

Fig. 7 - Calculated stacking fault states (dashed lines) for the ISF.

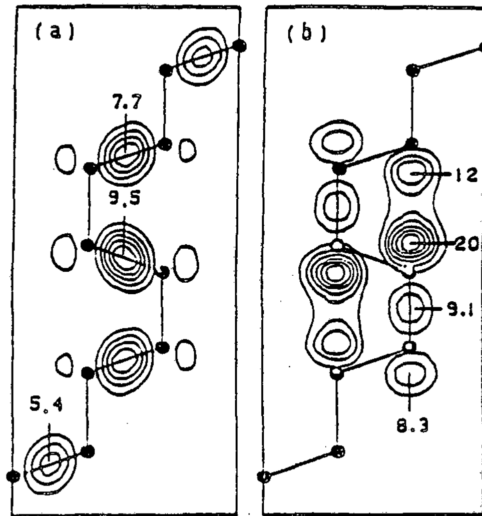

Fig. 8 - Charge density of stacking fault states of the ISF at Γ with energies (a) 0.1 eV above the valence band maximum and (b) 0.3 eV below the conduction band minimum. The charge density is in units of electron per cell volume and is normalized to one electron per cell. The contour intervals are (a) 1.5 and (b) 3.0.

(Fig. 8(b)). Similar stacking fault states are found for the ESF.

V - SUMMARY

We have presented a review of the *ab initio* pseudopotential density functional method for studying surfaces and interfaces. Results from calculations on the diamond (111) surface and the stacking faults in Si are discussed. For the case of the diamond surface, the bonding properties and structure of the 2x1 reconstruction are examined. A fully relaxed π-bonded geometry is predicted from total energy minimization. For the case of stacking faults, calculations are carried out for extrinsic and intrinsic faults along the [111] direction. The stacking fault energies are calculated, and forces on the atoms are determined for the ideal geometries. The existence and the properties of localized defect states are also examined and compared with experiment. The only input to the calculations are the atomic numbers and a set of possible structural topologies.

Acknowledgement - This work was supported by National Science Foundation Grant No. DMR8319024 and by a program development fund from the Director of the Lawrence Berkeley Laboratory under Contract No. DE-AC03-76SF00098.

References

[1] For a recent review, see M. L. Cohen, Advances in Electronics and Electron Physics, Vol. 51, eds. L. Marton and C. Marton, Academic Press, New York, pp. 1-62 (1980).
[2] S. G. Louie, Proceedings of NATO Advanced Study Institute on Electronic Structure, Dynamics and Quantum Structural Properties of Condensed Matter, 1984, eds. J. T. Devreese, P. E. Van Camp, and H. Nachtegaele, Plenum Press (in press) and references therein.
[3] D. Vanderbilt and S. G. Louie, Phys. Rev. B 29, 7099 (1984).
[4] M. Y. Chou, S. G. Louie, and M. L. Cohen, Proceedings of the 17th International Conference on the Physics of Semiconductors, 1984, eds. D. J. Chadi and W. A. Harrison, Springer-Verlag (in press).
[5] P. Hohenberg and W. Konn, Phys. Rev. 136, B864 (1964).
[6] W. Kohn and L. J. Sham, Phys. Rev. 140, A1133 (1965).
[7] J. Ihm, A. Zunger, and M. L. Cohen, J. Phys. C 12, 4401 (1979).
[8] M. L. Cohen and S. G. Louie, Ann. Rev. Phys. Chem. 35, 537 (1984).
[9] S. G. Louie and M. L. Cohen, Phys. Rev. Lett. 35, 866 (1975); Phys. Rev. B 13, 2461 (1976).
[10] A. Thanailakis, J. Phys. C 8, 655 (1975).
[11] J. Bardeen, Phys. Rev. 71, 717 (1947); V. Heine, Phys. Rev. 138, A1689 (1965).
[12] S. G. Louie, J. R. Chelikowsky, and M. L. Cohen, Phys. Rev. B 15, 2154 (1977).
[13] J. R. Chelikowsky and S. G. Louie, Phys. Rev. B 29, 3470 (1984).
[14] F. J. Himpsel, D. E. Eastman, P. Heimann, and J. F. van der Veen, Phys. Rev. B 24, 7270 (1981).
[15] B. B. Pate et al., J. Vac. Sci. Technol. 19, 349 (1981).
[16] S. V. Pepper, Surf. Sci. 12, 47 (1982).
[17] W. S. Yang and F. Jona, Phys. Rev. B 29, 899 (1984).

[18] D. Haneman, Phys. Rev. 121, 1093 (1961).
[19] K. C. Pandey, Phys. Rev. Lett. 47, 1913 (1981); Phys. Rev. B 25, 4338 (1982).
[20] D. J. Chadi, Phys. Rev. B 26, 4762 (1982).
[21] R. Seiwatz, Surf. Sci. 2, 473 (1964).
[22] The ideal Pandey π-bonded chain model is defined as having all bulk bond lengths except for graphite-length bonds along the surface chains.
[23] J. E. Northrup and M. L. Cohen, Phys. Rev. Lett. 49, 1349 (1982); Phys. Rev. B 27, 6553 (1983).
[24] I. L. F. Ray and D. J. H. Cockayne, Proc. R. Sco. London A 325, 543 (1971).
[25] H. Foll and C. B. Carter, Phil. Mag. A 40, 497 (1979).
[26] L. C. Kimerling, H. J. Leamy, and J. R. Patel, Appl. Phys. Lett. 30, 217 (1977).
[27] E. R. Weber and H. Alexander, J. de Phys. (Colloque) C 4, 319 (1983).
[28] C. Weigel, H. Alexander, and J. W. Corbett, Phys. Status Solidi B 71, 701 (1975).
[29] L. F. Mattheiss and J. R. Patel, Phys. Rev. B 23, 5384 (1981).
[30] J. Sanchez-Dehesa, J. A. Verges, and C. Tejedor, Phys. Rev. B 24, 1006 (1981).

This report was done with support from the Department of Energy. Any conclusions or opinions expressed in this report represent solely those of the author(s) and not necessarily those of The Regents of the University of California, the Lawrence Berkeley Laboratory or the Department of Energy.

Reference to a company or product name does not imply approval or recommendation of the product by the University of California or the U.S. Department of Energy to the exclusion of others that may be suitable.

LAWRENCE BERKELEY LABORATORY
TECHNICAL INFORMATION DEPARTMENT
UNIVERSITY OF CALIFORNIA
BERKELEY, CALIFORNIA 94720